Inorg. Chem. **2009**, *48*, 681−686

Template-Based Fabrication of $SrTiO_3$ and $BaTiO_3$ Nanotubes

Ying-Yu Chen,[†] Bang-Ying Yu,[†] Jung-Hui Wang,[†] Rebecca E. Cochran,[†] and Jing-Jong Shyue*[,†,‡]

Research Center for Applied Sciences, Academia Sinica, Taipei 115, and Department of Materials Science and Engineering, National Taiwan University, Taipei 106, Taiwan 106, Republic of China

Received October 3, 2008

In response to the growing need for metal oxide nanotubes and nanowires for nanoelectronic applications, polycrystalline titanate nanotubes are synthesized in this work at near-ambient conditions without the application of an external electric field or pre-existing solids. Nanotubes of complicated metal oxides including strontium titanate and barium titanate are fabricated inside anodic aluminum oxide (AAO) templates from aqueous solutions using a simple, inexpensive, reproducible, and environmentally friendly procedure. The deposition solution is prepared by dissolving ammonium hexafluorotitanate and strontium nitrate in a boric acid solution at a pH of 2.5. The typical lengths of $SrTiO_3$ nanotubes are 5−30 μm, with an average diameter of approximately 250 nm, which is defined by the pore diameter of the AAO template. After annealing at 800 °C in air, the resulting nanotubes are polycrystalline cubic $SrTiO_3$. The Sr:Ti ratio in the nanotube is controlled by the hydrolysis of TiF_6^{2-} ions, and the concentration of Sr^{2+} and stoichiometric $SrTiO_3$ nanotubes can be obtained. As an additional controlling factor, the surface properties of the AAO can be modified by (octadecyl)trichlorosilane. Barium titanate is also prepared in a similar manner with barium nitrate and ammonium hexafluorotitanate as precursors. The polycrystalline cubic $BaTiO_3$ nanotubes are 12−30 μm long and approximately 250 nm in diameter.

Introduction

Metal oxide nanotubes are being increasingly used as building blocks in multifunctional "bottom up" nanoelectronics by taking advantage of the myriad of size-dependent properties of metal oxides, such as electrical conductivity,[1] ferroelectric effects,[2] piezoelectric effects,[3] electro-optic effects,[4] chemical sensing,[1,5−7] and magnetoresistance.[8] Many methodologies have been developed to synthesize one-dimensional structures. A majority of these methods require high temperatures, high pressures, vacuum, and/or externally applied electric fields. Nanofabrication by self-organization methods using porous templates has drawn much attention due to the fact that it enables mass production without the introduction of expensive lithographical tools or application of extreme conditions such as electron beam exposure or ultrahigh vacuum.[4,9−13]

Recently, for ease of processing, anodic aluminum oxide (AAO) has been widely used as a structure-directing template to form one-dimensional nanomaterials, such as polymers,[14,15] liquid crystals,[14,15] metals,[16−18] and metal ox-

* To whom correspondence should be addressed. Phone +866(2)2789-8000#69. E-mail: shyue@gate.sinica.edu.tw.
† Academia Sinica.
‡ National Taiwan University.

(1) Shyue, J. J.; Cochran, R. E.; Padture, N. P. *J. Mater. Res.* **2006**, *21*, 2894–2903.
(2) Yun, W. S.; Urban, J. J.; Gu, Q.; Park, H. *Nano Lett.* **2002**, *2*, 447–450.
(3) Wang, Z. L.; Song, J. H. *Science* **2006**, *312*, 242–246.
(4) Xia, Y.; Yang, P.; Sun, Y.; Wu, Y.; Mayers, B.; Gates, B.; Yin, Y.; Kim, F.; Yan, H. *Adv. Mater.* **2003**, *15*, 353–389.
(5) Cochran, R. E.; Shyue, J. J.; Padture, N. P. *Acta Mater.* **2007**, *55*, 3007–3014.
(6) Kolmakov, A.; Moskovits, M. *Annu. Rev. Mater. Res.* **2004**, *34*, 151–180.
(7) Kolmakov, A.; Zhang, Y. X.; Cheng, G. S.; Moskovits, M. *Abstr. Pap.—Am. Chem. Soc.* **2003**, *225*, U522.
(8) Terrier, C.; Abid, M.; Arm, C.; Serrano-Guisan, S.; Gravier, L.; Ansermet, J. P. *J. Appl. Phys.* **2005**, *98*, 086102.
(9) Hulteen, J. C.; Martin, C. R. *J. Mater. Chem.* **1997**, *7*, 1075–1087.
(10) Lai, M.; Riley, D. J. *J. Colloid Interface Sci.* **2008**, *323*, 203–212.
(11) Lin, Y. S.; Kumakiri, I.; Nair, B. N.; Alsyouri, H. *Sep. Purif. Methods* **2002**, *31*, 229–379.
(12) Martin, C. R. *Science* **1994**, *266*, 1961–1966.
(13) Martin, C. R.; Vandyke, L. S.; Cai, Z. H.; Liang, W. B. *J. Am. Chem. Soc.* **1990**, *112*, 8976–8977.
(14) Steinhart, M.; Zimmermann, S.; Goring, P.; Schaper, A. K.; Gosele, U.; Weder, C.; Wendorff, J. H. *Nano Lett.* **2005**, *5*, 429–434.
(15) Steinhart, M.; Murano, S.; Schaper, A. K.; Ogawa, T.; Tsuji, M.; Gosele, U.; Weder, C.; Wendorff, J. H. *Adv. Funct. Mater.* **2005**, *15*, 1656–1664.
(16) Yanagishita, T.; Nishio, K.; Masuda, H. *Adv. Mater.* **2005**, *17*, 2241–2243.
(17) Yoo, W. C.; Lee, J. K. *Adv. Mater.* **2004**, *16*, 1097.
(18) Masuda, H.; Fukuda, K. *Science* **1995**, *268*, 1466–1468.

10.1021/ic8018887 CCC: $40.75
Published on Web 12/16/2008

ides[1,5,19] (for recent reviews on template-based synthesis of metal nanowires and oxide nanowire, see refs 20 and 21, respectively). At near-ambient conditions, the AAO-based general method for preparing 1D metal oxides consists of electroplating materials in the confined space followed by selective oxidation[22−24] or filling the template with pre-existing nanoparticles prepared by the sol−gel technique using electrophoresis or dip-casting.[25−27] In other words, these methods consist of multiple processing steps including the thermoevaporation of electrodes followed by electroplating or fabrication of nanoparticles before dip-casting.

Using AAO as a template, we previously demonstrated that crystalline nanotubes and nanowires of metal oxides, including TiO_2, ZrO_2, SnO_2, FeOOH, and core−shell TiO_2−ZrO_2, can be synthesized at near-ambient conditions without the application of heat treatment, external electric fields, or pre-existing ceramic particles.[1,28] Nevertheless, complicated functional oxides such as titanates have not been fabricated using this single-step, low-cost method. This method is based on liquid-phase deposition (LPD)[29−33] from chemical solutions, which has been successfully used to deposit a wide variety of crystalline oxides in the form of thin films on flat substrates. By adding a secondary cation to the deposition solution, oxide thin films with two cations can be deposited[34−37] so that complicated oxide nanotubes can be fabricated in a similar manner. The advantages of this near-ambient method for synthesizing metal oxide nanotubes are minimal equipment requirements, low cost, and possible incorporation of biomolecules and temperature-sensitive moieties.

In this work, complicated oxides, including $SrTiO_3$ and $BaTiO_3$, were deposited as nanotubes using AAO as a template under near-ambient conditions without external electric fields or pre-existing solids. As hydrophobicity is an additional factor that can affect the deposition of titanate, AAO was optionally modified with (octadecyl)trichlorosilane (OTS). The effects of precursor concentration, pH, and deposition temperature were also examined to optimize the deposition conditions for preparing stoichiometric oxides. The as-prepared oxides with a stoichiometric ratio were found to be amorphous and can be crystallized to the polycrystalline cubic phase after annealing.

Scheme 1. IEPs of the Species Presented in This Work and Their Surface Charge[a]

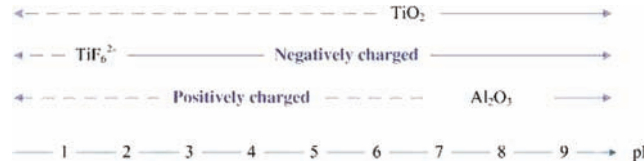

[a] The broken lines and solid lines indicate the pH range where the species are positively and negatively charged, respectively.

Experimental Section

AAO Templates. On the basis of commercially available filtration membranes (Whatman, Anodisc 47, England; ~60 μm in thickness, approximately 250 nm in pore diameter), two types of AAO templates with different surface properties were used. With native surface hydroxyl groups, the as-received AAO is hydrophilic and readily used for deposition. The AAO membranes were also modified with OTS (Acros) to make the surface hydrophobic in an effort to study the effect of surface hydrophobicity on nanotube deposition. The modification was accomplished by placing the AAO templates in slowly stirred 1% (v/v) OTS in bicyclohexyl (BCH; Acros) for 24 h. The AAO templates were then removed from the solution, rinsed with chloroform, and then air-dried at room temperature.

Synthesis of Titanate Nanotubes. A liquid-phase deposition[29−33] based process was used to fabricate $SrTiO_3$ nanotubes. In short, ammonium hexafluorotitanate ($(NH_4)_2TiF_6$; 5.0−20 mM, Acros) and strontium nitrate ($Sr(NO_3)_2$; 1−20 mM, Showa, Japan) were dissolved in an aqueous solution of boric acid (Tedia; fixed at 3 times the concentration of $(NH_4)_2TiF_6$ at room temperature. The pH was adjusted by adding 1.0 M HCl dropwise. Similarly, barium titanate ($BaTiO_3$) nanotubes were synthesized. The only difference from the synthesis of $SrTiO_3$ was that $Sr(NO_3)_2$ was replaced by barium nitrate ($Ba(NO_3)_2$; 0.5−20 mM, Showa, Japan).

The AAO membranes were immersed in the precursor solutions and held at specific temperatures (23−80 °C) in an oil bath for 20 h. The AAO templates were then removed from the solutions and rinsed with deionized water. The nanotubes were released by dissolving the AAO templates in 1 M NaOH aqueous solution with ultrasonic agitation, and then the solid was collected by centrifuge (Hettich, Universal 320, Germany; 15 000 rpm, relative centrifugal force (RCF) 40 240) for 2 min. The dissolution and collection steps were repeated two more times to fully remove the AAO templates. The nanotubes were then washed in deionized water three times to remove remaining ions. Purified nanotubes were annealed in a furnace (BF51848C-1, Lindberg/Blue) at 800 °C for 3 h with a temperature ramping rate of 4 °C/min in air. The tubes were then dispersed in ethanol for further analysis.

The titanates synthesized in this work are labeled *w*Sr*x*Ti*y*°C*z*h or *w*Ba*x*Ti*y*°C*z*h, where *w*, *x*, *y*, and *z* denote the concentration of

(19) Limmer, S. J.; Seraji, S.; Wu, Y.; Chou, T. P.; Nguyen, C.; Cao, G. Z. *Adv. Funct. Mater.* **2002**, *12*, 59–64.
(20) Kline, T. R.; Tian, M.; Wang, J.; Sen, A.; Chan, M. W. H.; Mallouk, T. E. *Inorg. Chem.* **2006**, *45*, 7555–7565.
(21) Bae, C.; Yoo, H.; Kim, S.; Lee, K.; Kim, J.; Sung, M. M.; Shin, H. *Chem. Mater.* **2008**, *20*, 756–767.
(22) Tresback, J. S.; Vasiliev, A. L.; Padture, N. P. *J. Mater. Res.* **2005**, *20*, 2613–2617.
(23) Herderick, E. D.; Tresback, J. S.; Vasiliev, A. L.; Padture, N. P. *Nanotechnology* **2007**, *18*, 155204.
(24) Tresback, J. S.; Vasiliev, A. L.; Padture, N. P.; Park, S.-Y.; Berger, P. R. *IEEE Trans. Nanotechnol.* **2007**, *6*, 676–681.
(25) Hernandez, B. A.; Chang, K.-S.; Fisher, E. R.; Dorhout, P. K. *Chem. Mater.* **2002**, *14*, 480–482.
(26) Cheng, B.; Samulski, E. T. *J. Mater. Chem.* **2001**, *11*, 2901–2902.
(27) Gasparac, R.; Kohli, P.; Mota, M. O.; Trofin, L.; Martin, C. R. *Nano Lett.* **2004**, *4*, 513–516.
(28) Shyue, J. J.; Padture, N. P. *Mater. Lett.* **2007**, *61*, 182–185.
(29) Deki, S.; Aoi, Y.; Asaoka, Y.; Kajinami, A.; Mizuhata, M. *J. Mater. Chem.* **1997**, *7*, 733–736.
(30) Koumoto, K.; Seo, S.; Sugiyama, T.; Seo, W. S. *Chem. Mater.* **1999**, *11*, 2305–2309.
(31) Deki, S.; Aoi, Y.; Yanagimoto, H.; Ishii, K.; Akamatsu, K.; Mitzuhata, M.; Kajinami, A. *J. Mater. Chem.* **1996**, *6*, 1879–1882.
(32) Nagayama, H.; Honda, H.; Kawahara, H. *J. Electrochem. Soc.* **1988**, *135*, 2013–2016.
(33) Kishimoto, H.; Takahama, K.; Hashimoto, N.; Aoi, Y.; Deki, S. *J. Mater. Chem.* **1998**, *8*, 2019–2024.
(34) Gao, Y. F.; Masuda, Y.; Yonezawa, T.; Koumoto, K. *Mater. Sci. Eng., B* **2003**, *99*, 290–293.
(35) Gao, Y. F.; Masuda, Y.; Koumoto, K. *Chem. Mater.* **2003**, *15*, 2399–2410.
(36) Gao, Y. F.; Masuda, Y.; Koumoto, K. *Electroceram. Jpn. VI* **2003**, *248*, 73–76.
(37) Gao, Y. F.; Masuda, Y.; Yonezawa, T.; Koumoto, K. *Chem. Mater.* **2002**, *14*, 5006–5014.

$Sr(NO_3)_2$ or $Ba(NO_3)_2$, concentration of $(NH_4)_2TiF_6$, deposition temperature, and deposition time, respectively.

Characterization. Scanning electron microscopy (SEM; FEI Nova NanoSEM200) was used to observe the deposition behavior and determine the length of the tubes. Because of the low conductivity of the AAO, the microscope was operated in low-vacuum mode (0.08−0.23 Torr) without a conductive overcoat. X-ray photoelectron spectroscopy (XPS; PHI VersaProbe5000, Chigasaki, Japan) was used to determine the chemical composition of the specimen with a microfocused (100 μm, 25 W) monochromatic Al Kα X-ray and 45° photoelectron takeoff angle. Transmission electron microscopy (TEM) specimens were prepared by dispersing the purified nanotubes on carbon-foam-coated copper grids. The nanotubes were examined with a Jeol JEM-1230 operated at 100 kV and a JEM-2100F operated at 200 kV.

Results and Discussion

$SrTiO_3$ Nanotubes. To deposit $SrTiO_3$ nanotubes in AAO templates, the effect of the pH of the deposition solution was first examined. At a pH of 5.0, the precursor solution (15Sr15Ti) turned into a gel. Large grains were observed megascopically, and the viscosity became higher with increasing pH. At this pH, nothing was deposited inside the pores of the AAO due to large particles sealing the opening of the pore. Nevertheless, nanotubes were successfully deposited at pH 2.5 and below. To understand the mechanism and the effect of pH, the chemical reactions must be considered. $(NH_4)_2TiF_6$ and $Sr(NO_3)_2$ were used as precursors, which dissociated to TiF_6^{2-} and Sr^{2+} ions in the aqueous solution. The expected reactions are as follows:

$$TiF_6^{2-}(aq) + Sr^{2+}(aq) + 3H_2O(l) \rightleftharpoons SrTiO_3(s) + 6H^+(aq) + 6F^-(aq) \quad (1)$$

$$H_3BO_3(aq) + 4F^-(aq) + 3H^+(aq) \rightleftharpoons BF_4^-(aq) + 3H_2O(l) \quad (2)$$

where the boric acid scavenges F^-, promoting reaction 1. Furthermore, for the hydrolysis of TiF_6^{2-} and Sr^{2+}, reactions 3 and 4 can be discussed separately as follows:

$$TiF_6^{2-}(aq) + 2H_2O(l) \rightleftharpoons TiO_2(s) + 4H^+(aq) + 6F^-(aq) \quad (3)$$

$$Sr^{2+}(aq) + H_2O(l) \rightleftharpoons SrO(s) + 2H^+(aq) \quad (4)$$

Clearly, H^+ inhibits these reactions by shifting the equilibrium to the left-hand side. In addition, the kinetics of these reactions are slower at low pH. In other words, high pH yields excess hydrolysis. It is responsible not only for large-sized grains blocking the pores but also for deposition outside the template that leads to a low yield of nanotubes. To slow the hydrolysis of TiF_6^{2-} and Sr^{2+} in the solution and maintain stable deposition conditions, lower pH is desired. Moreover, the reactions for $BaTiO_3$ synthesis are similar to reactions 1−4, replacing Sr^{2+} with Ba^{2+}.

Besides stable hydrolysis in the deposition solution, the other critical factor for depositing materials in the template is the interaction between the ions/clusters in the solution and the substrate. When an AAO template is immersed in the precursor solution, the chemistry of the solution is critical for deposition inside the confined space. In particular, electrostatic interactions between the species are known to control the deposition of materials.[38−41] For the deposition to occur, metal-containing clusters have to be adsorbed by the surface of the AAO membrane through electrostatic interaction, and the surface charge is known to be controlled by the pH through the hydrolysis of cations. To have strong attractive interaction, which leads to a higher yield of deposition, the ionic behaviors of SrO, BaO, TiO_2, and Al_2O_3 are considered.

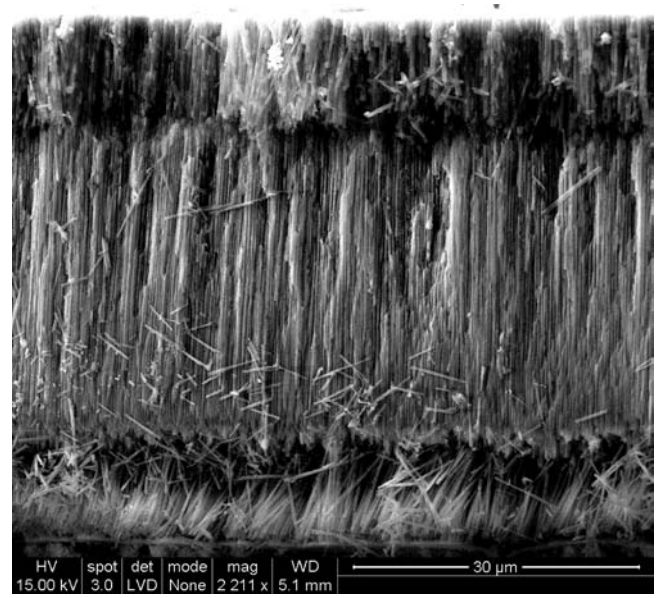

Figure 1. A cross-sectional SEM micrograph of an AAO template after the deposition of $SrTiO_3$ nanotubes (8Sr8Ti45°C20h).

Table 1. Relation between Precursor Concentrations and Sr:Ti Elemental Composition in the Solid

	OTS modification	Sr:Ti atomic ratio	tube length (μm)
5Sr5Ti45°C20h	no	0.24	10
8Sr8Ti45°C20h	no	0.45	15
15Sr15Ti45°C20h	no	0.91	4.0
15Sr15Ti45°C20h	yes	0.86	12
20Sr20Ti45°C20h	yes	1.07	>30

The isoelectric point (IEP) is the pH at which the total surface charge is zero. When the environmental pH is lower than the IEP, the surface is positively charged. The IEPs of TiO_2 and Al_2O_3 are known to be at 6−7[42] and 7−9,[42] respectively. Scheme 1 shows the pH-dependent surface charge of species presented in this work. Only when species are charged oppositely are they electrostatically attracted to each other. In general, the IEPs of TiO_2 and Al_2O_3 are close so that electrostatic repulsion between Ti- and Al-containing species is expected. In other words, Ti-containing species cannot be deposited on the AAO membrane. In the context

(38) Shyue, J. J.; Tang, Y.; De Guire, M. R. *J. Mater. Chem.* **2005**, *15*, 323–330.
(39) Shyue, J. J.; De Guire, M. R. *J. Am. Chem. Soc.* **2005**, *127*, 12736–12742.
(40) Shyue, J. J.; De Guire, M. R. *Chem. Mater.* **2005**, *17*, 5550–5557.
(41) Shyue, J. J.; De Guire, M. R. *Langmuir* **2004**, *20*, 8693–8698.
(42) Reed, J. S. *Principles of Ceramics Processing*, 2nd ed.; John Wiley & Sons: New York, 1995.

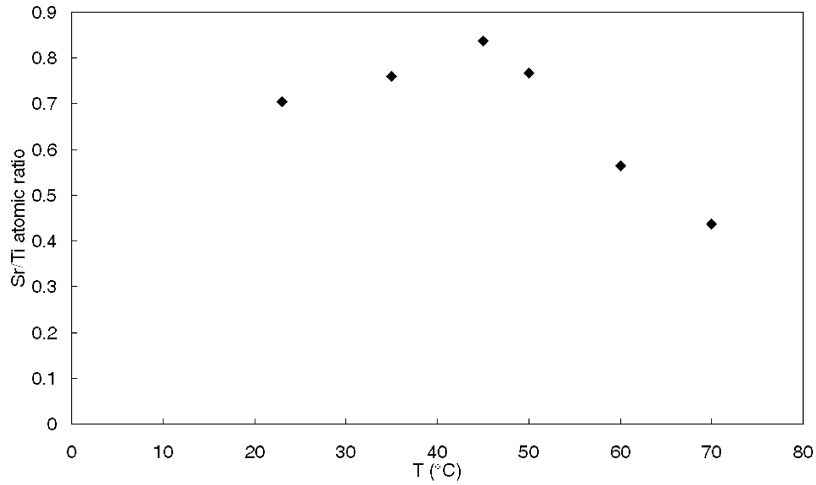

Figure 2. Sr:Ti atomic ratio of the nanotubes deposited at a temperature range of 23−70 °C.

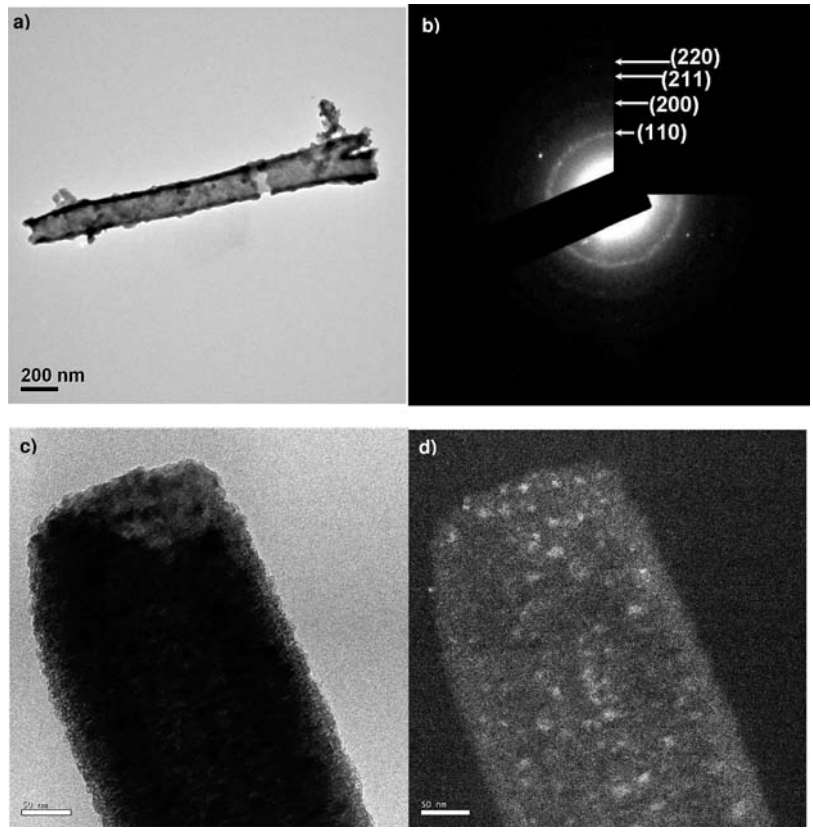

Figure 3. (a) Bright-field TEM images of an isolated $SrTiO_3$ nanotube (15Sr15Ti45°C20h). (b) Indexed electron diffraction pattern of the nanotube. (c) Bright-field and (d) dark-field TEM images near the opening of the nanotube.

of chemical deposition of thin films, it has been shown that the use of the $(NH_4)_2TiF_6$ precursor results in Ti-containing clusters with a much lower IEP (pH $\approx$ 1.5).[43] Therefore, starting with $(NH_4)_2TiF_6$, Ti-containing species are expected to be deposited on AAO templates between pH 1.5 and pH 7.0.

With high solubility, Sr- and Ba-containing species are expected to be positively charged at this range of pH. Therefore, SrO and BaO cannot be deposited on AAO directly. Nevertheless, the negatively charged Ti-containing cluster can attract Sr^{2+} and Ba^{2+}, hence acting as a seed for depositing Sr- and Ba-containing species on AAO. This kind of codeposition phenomenon has also been reported in titanium−vanadium oxides where the Ti and V species attract each other, forming near-neutral species before being deposited on the substrate.[40,44]

In summary, lower pH is desired to slow the hydrolysis of fluorotitanate in the solution, maintain stable deposition conditions, and have a strong attraction between Ti-containing clusters, AAO, and IIA cations. However, consisting of

(43) Masuda, Y.; Sugiyama, T.; Seo, W. S.; Koumoto, K. *Chem. Mater.* **2003**, *15*, 2469–2476.

(44) Shyue, J. J.; De Guire, M. R. *Trans. Mater. Res. Soc. Jpn.* **2004**, *29*, 2383–2386.

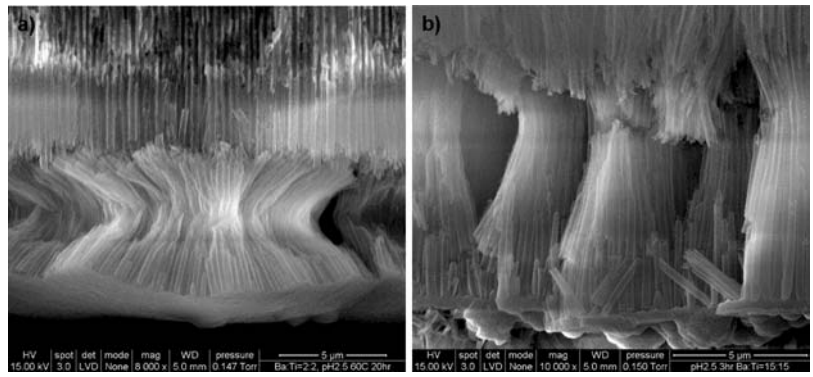

Figure 4. Cross-sectional SEM micrographs of $BaTiO_3$ nanotubes deposited in AAO templates from (a) 2 mM and (b) 15 mM precursor concentration.

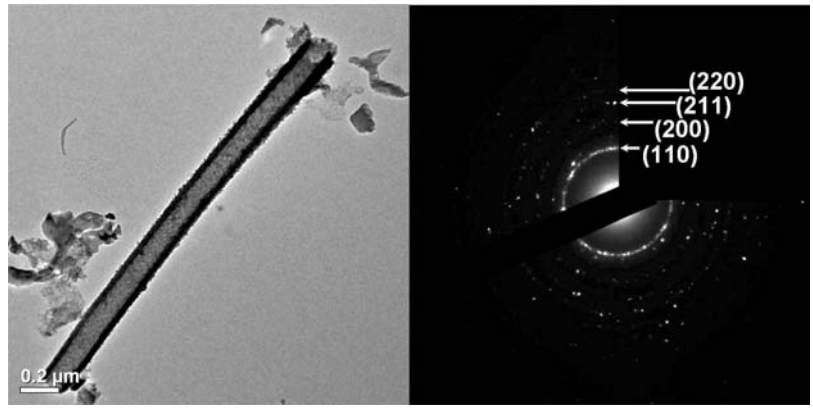

Figure 5. Bright-field TEM images and indexed electron diffraction pattern of an isolated $BaTiO_3$ nanotube (2Ba2Ti60°C20h).

Al_2O_3, AAO can be dissolved at low pH. Therefore, a pH of 2.5 is selected because it is slightly above the pH where damage to AAO is clearly observed (pH 2.0). Figure 1 reveals the frayed nanotubes inside the AAO (8Sr8Ti45°C20h). Uniformly sized nanotubes approximately 250 nm in diameter and 15 μm in length were grown over large areas on the AAO template.

It is expected that by altering the ratio of Sr and Ti precursor in the deposition solution, the deposited solid will have a different cation ratio. Precursor ratios of $Sr(NO_3)_2$ to $(NH_4)_2TiF_6$ between 0.10 and 10 at a pH of 2.5 were examined in this work. It was found that $SrTiO_3$ nanotubes were deposited in AAO templates only when the Sr^{2+}:TiF_6^{2-} ratio was near unity. When the concentration of Sr^{2+} is higher than that of TiF_6^{2-}, the deposition does not occur. Considering the high solubility of Sr^{2+} and that the AAO would repel positively charged Sr clusters, it is difficult for Sr-containing species to be deposited directly. In addition, with the low concentration of TiF_6^{2-}, the solution contained an inadequate amount of negatively charged Ti-containing clusters that can be deposited in AAO, because these clusters will be attracted by excess Sr^{2+} ions in the solution and lose their negative charges. As a result, deposition in the AAO did not occur. On the other hand, when $(NH_4)_2TiF_6$ was more concentrated than $Sr(NO_3)_2$, excess TiF_6^{2-} led to competing TiO_2 tubes growing in the AAO template instead of $SrTiO_3$ because there was not enough Sr^{2+} in the solution.

The effect of the precursor concentration was also studied. It was observed that $SrTiO_3$ nanotubes were successfully deposited over a large area in the AAO template while the precursor concentrations (1:1) were between 5 and 15 mM. In addition, the tube wall was thicker with more concentrated precursors due to the faster hydrolysis of cations. The elemental composition of the nanotubes was determined by XPS after being released from the AAO templates. Table 1 lists the chemical compositions and tube lengths of nanotubes prepared from different precursor concentrations. With higher concentrations, the chemical composition is closer to stoichiometric $SrTiO_3$. This change in composition can be attributed to the high solubility of Sr^{2+} in the solution; i.e., a high concentration was required for Sr to be present in the solid phase. However, when the concentration was higher than 15 mM, the fast hydrolysis of TiF_6^{2-} caused a high deposition rate at the opening of AAO pores. As a result, the pores were blocked, which prevented precursor transport into the pore. Therefore, nanotubes became shorter at higher concentration (15 μm from 8 mM and 4 μm from 15 mM precursor solution) and were not observed at precursor concentrations higher than 15 mM.

To further increase the Sr content in the solid by increasing the precursor concentration and to slow the deposition kinetics on the AAO, an OTS-modification pretreatment was introduced. While OTS is hydrophobic and inhibits the deposition, it is slowly removed during the course of oxide deposition, allowing the deposition to take place.[5] As a result, the overall deposition rate decreased and the pore blocking was suppressed. Using the OTS modification, the tube length was 12 μm, which is much longer than that without OTS modification (4 μm) under the same deposition conditions

(15Sr15Ti45°C20h). On the basis of the OTS-modification method, longer and more stoichiometric $SrTiO_3$ nanotubes were fabricated with 20 mM precursor concentration.

Aside from the pH and precursor concentration, the other factor that could change the kinetics of hydrolysis, and hence change the chemical composition, is the temperature. Figure 2 shows the Sr:Ti ratio of the nanotube deposited at different temperatures (15Sr15Ti with OTS modification). At temperatures below 50 °C, the Sr concentration increased slightly with the temperature. However, at higher temperatures, because the hydrolysis of TiF_6^{2-} becomes faster than that of Sr^{2+} and the solubility of Sr^{2+} increases with temperature, Ti-enriched nanotubes were observed.

Although crystalline $SrTiO_3$ thin films have been deposited using similar solution chemistry,[34,45] as-prepared nanotubes confined in AAO templates were found to be amorphous. To crystallize the nanotubes, the specimen was heat-treated at 800 °C for 3 h in air after the nanotubes were released from the template. TEM (Figure 3a) shows the $SrTiO_3$ nanotubes approximately 250 nm in diameter and about 2 μm in length (15Sr15Ti45°C20h). Figure 3b shows the electron diffraction pattern of the tube. The diffraction pattern indicated cubic phase $SrTiO_3$ (PDF no. 84-0443); phase-separated SrO and TiO_2 were not observed. The grain size is about 10 nm (Figure 3c,d). The length observed in TEM was a little shorter than the length observed in SEM owing to the tubes breaking during the ultrasonic cleaning.

$BaTiO_3$ Nanotubes. For the preparation of $BaTiO_3$ nanotubes, the solution chemistry is expected to be similar to that of $SrTiO_3$ nanotube synthesis because the hydrolysis of Ba^{2+} is similar to that of Sr^{2+}. The deposition pH was tuned to 2.5, and the precursor ratio was set to 1. The observed effect of the precursor concentrations in this system was similar to that of $SrTiO_3$; i.e., the higher the precursor concentration, the higher the Ba:Ti atomic ratio (0.23 and 0.84 with 2.0 and 15 mM precursors, respectively; 0.95 with 15 mM precursor and OTS modification). Figure 4 shows SEM micrographs of the nanotubes prepared in different deposition conditions. In both deposition conditions, $BaTiO_3$ tubes were deposited uniformly with a width of approximately 250 nm over large areas in the AAO template. It was noted that nanotubes with thinner tube walls were fabricated with 2 mM precursor solution due to slower hydrolysis of cations, which is similar to the fabrication of $SrTiO_3$ in low-concentration regions.

Purified nanotubes were analyzed in TEM after being released from the AAO templates and annealed in air at 800 °C for 3 h. Figure 5 shows the $BaTiO_3$ nanotubes (2Ba2Ti60°C20h) with diameters of approximately 250 nm and lengths of 2.5 μm, which was consistent with the SEM observation. The electron diffraction pattern of the tube indicated that the $BaTiO_3$ nanotubes were polycrystalline cubic phase (PDF no. 86-0177).

Conclusion

On the basis of liquid-phase deposition, complicated oxides including $SrTiO_3$ and $BaTiO_3$ nanotubes were fabricated using anodic aluminum oxide as a structure-directing template from aqueous solutions. The deposition mechanism of titanates in the confined space was elucidated. It was found that the deposition is mainly controlled by the hydrolysis of the TiF_6^{2-} precursor. Positively charged Sr^{2+} or Ba^{2+} ions are then attracted by the negatively charged Ti cluster and deposited on the positively charged AAO surface. Titanate nanotubes can only be deposited when the precursor ratio is close to unity. The effect of pH was discussed and optimized at 2.5 for the synthesis. The cation ratio in the solid phase is controlled by the precursor concentration, and it was found that high concentration leads to stoichiometric titanates. To suppress the deposition at the opening of the pore, OTS-modified AAO templates were also used. With the OTS modification, stoichiometric $SrTiO_3$ nanotubes with lengths exceeding 30 μm were fabricated. The advantages of this near-ambient method for synthesis of crystalline metal oxide nanotubes are minimal equipment requirements, low cost, and possible incorporation of biomolecules and temperature-sensitive moieties.

Acknowledgment. We acknowledge the sponsorship by Academia Sinica and the Taiwan National Science Council through Grant Number 96-2113-M-001-012-MY2.

IC8018887

(45) Gao, Y. F.; Masuda, Y.; Peng, Z. F.; Yonezawa, T.; Koumoto, K. *J. Mater. Chem.* **2003**, *13*, 608–613.